



ARTICLE

Factors that influence the thymic selection of CD8 $\alpha\alpha$ intraepithelial lymphocytesNadia S. Kurd^{1,2}, Ashley Hoover^{1,3}, Jaewon Yoon¹, Brian M. Weist^{1,4}, Lydia Lutes¹, Shiao Wei Chan¹ and Ellen A. Robey¹

Thymocytes bearing $\alpha\beta$ T cell receptors (TCR $\alpha\beta$) with high affinity for self-peptide-MHC complexes undergo negative selection or are diverted to alternate T cell lineages, a process termed agonist selection. Among thymocytes bearing TCRs restricted to MHC class I, agonist selection can lead to the development of precursors that can home to the gut and give rise to CD8 $\alpha\alpha$ -expressing intraepithelial lymphocytes (CD8 $\alpha\alpha$ IELs). The factors that influence the choice between negative selection versus CD8 $\alpha\alpha$ IEL development remain largely unknown. Using a synchronized thymic tissue slice model that supports both negative selection and CD8 $\alpha\alpha$ IEL development, we show that the affinity threshold for CD8 $\alpha\alpha$ IEL development is higher than for negative selection. We also investigate the impact of peptide presenting cells and cytokines, and the migration patterns associated with these alternative cell fates. Our data highlight the roles of TCR affinity and the thymic microenvironments on T cell fate.

Mucosal Immunology (2021) 14:68–79; <https://doi.org/10.1038/s41385-020-0295-5>

INTRODUCTION

During development, thymocytes are tested for the ability of their T cell receptor (TCR) to recognize self-peptide bound to Major Histocompatibility Complex (MHC) proteins. While low to moderate self-reactivity is required for maturation and CD4/CD8 lineage commitment (positive selection), cells with high self-reactivity must be either deleted (negative selection) or diverted into alternate T cell lineages in order to maintain self-tolerance. Lineage diversion of self-reactive thymocytes (termed agonist selection)¹ has been extensively studied for thymic-derived T_{regs} (tT_{regs}) specific for MHC class II, and invariant natural killer T cells (iNK T cells) specific for the non-classical MHC I molecule CD1d. More recently, evidence has emerged that agonist selection by a variety of different MHC molecules, including classical and nonclassical MHC I and classical MHC II, can lead to the development of thymic precursors to intraepithelial lymphocytes (IEL) that express TCR $\alpha\beta$ and CD8 $\alpha\alpha$ (hereinafter referred to as CD8 $\alpha\alpha$ IELs)^{2–5}. Although the exact roles of CD8 $\alpha\alpha$ IELs remain unclear, there is evidence that they, together with other IEL populations including TCR $\alpha\beta$ ⁺ CD8 $\alpha\beta$ IEL derived from conventional CD8 T cells and TCR $\gamma\delta$ ⁺ IEL, help to maintain immune homeostasis and tolerance in the gut^{6–8}.

While both negative selection and agonist selection are directed by a strong TCR signal, the factors that specify these divergent fates remain unclear. One popular notion posits that the degree of TCR self-reactivity required for agonist selection is intermediate between positive and negative selection. However, current evidence suggests that repertoire of tT_{regs} is quite broad, and overlaps extensively with both conventional CD4 T cells, as well as with thymocytes undergoing negative selection^{9,10}. Early evidence that strong TCR signals in the thymus drive CD8 $\alpha\alpha$ IEL development came from mice expressing a defined MHC class I-specific TCR (OT-

l) along with transgenic expression of the agonist ligand by medullary thymic epithelial cells (RIPmOVA mice)⁴. Further evidence came from the observation that the absence of the costimulatory CD28-B7 axis inhibited the negative selection of superantigen-reactive thymocytes, and favored their diversion into the CD8 $\alpha\alpha$ IEL lineage¹¹. Recent studies using mice with monoclonal expression of TCRs cloned from endogenous CD8 $\alpha\alpha$ IELs provided evidence that CD8 $\alpha\alpha$ IEL precursors are found within a highly self-reactive thymocyte population enriched in thymocytes undergoing negative selection^{2,5}, and can include thymocytes restricted to class I and class II, as well as nonclassical, MHC molecules. Whether stronger TCR signals are required for CD8 $\alpha\alpha$ IEL development compared to negative selection remains unknown.

Another factor that can affect thymocyte fate is access to cytokines. For example, the related cytokines IL-2 and IL-15 play critical roles in the agonist selection of tT_{regs} and iNK T cells^{12–16}. CD8 $\alpha\alpha$ IEL precursors express CD122, a shared subunit of the IL-15 and IL-2 receptors, suggesting the ability to respond to these cytokines^{2,3,5,17}. Although IL-15 is important for the survival and maintenance of mature CD8 $\alpha\alpha$ IELs in the gut, its role in their thymic development is less clear^{8,18–20}. One challenge in addressing this question is the lack of unambiguous markers for thymic CD8 $\alpha\alpha$ IEL precursors. For example, thymic IELp are often identified as TCR signaled TCR $\alpha\beta$ ⁺ CD4[–]CD8[–] thymocytes, however this may exclude IEL precursors with intermediate levels of CD4 and CD8^{2,3,5,17}. In addition, NK1.1 is sometimes used to exclude iNKT cells from the “IELp” population, however this would also exclude subsets of IELp that express this marker^{3,17}. In addition, even after excluding iNKT cells and CD4 or CD8 expressing thymocytes, thymocytes defined as IEL precursors still exhibit considerable heterogeneity^{3,17,21}, and it is unclear what fraction of these cells are bone fide precursors of mature CD8 $\alpha\alpha$ IELs.

¹Division of Immunology and Pathogenesis, Department of Molecular and Cell Biology, University of California Berkeley, Berkeley, CA 94720, USA

Correspondence: Ellen A. Robey (erobey@berkeley.edu)

²Present address: Department of Medicine, University of California San Diego, San Diego, CA 92093, USA

³Present address: Oklahoma Medical Research Foundation, Oklahoma City, OK 73104, USA

⁴Present address: Gilead Sciences, Foster City, CA 94404, USA

Received: 23 August 2019 Revised: 19 March 2020 Accepted: 6 April 2020

Published online: 1 June 2020

Another unresolved question is the pattern of thymocyte motility and signaling during agonist selection. Previous studies have shown that negative selection is associated with migratory arrest and sustained TCR signals, whereas positive selection is associated with continued migration interspersed with pauses and transient TCR signals^{22,23}. We previously examined the motility of surviving thymocytes in a steady state model of tolerance to a class I MHC-specific tissue restricted self-antigen (OT-I TCR and RIPmOVA transgenic mice), and reported a confined migration pattern of autoreactive thymocytes within zones of ~30 microns diameter in the thymic medulla²⁴. While that study did not address the ultimate fate of the autoreactive thymocytes, it is possible that the surviving thymocytes were undergoing agonist selection within confinement zones. However, the TCR signaling and motility patterns associated with agonist selection have not yet been specifically addressed.

In this study, we investigated these questions by examining a synchronous wave of CD8 α IEL development in thymic tissue slice cultures. We and others have previously used this experimental system to examine positive selection, negative selection, T_{reg} development, and thymocyte migration^{22,23,25–32}. Here, we showed that thymocytes bearing a class I specific TCR (OT-I) undergo either negative selection or CD8 α IEL development when cultured on thymic slices in the presence of agonist ligand, and we used this system to investigate factors that influence whether autoreactive thymocytes undergo death or agonist selection. We found that higher affinity TCR signals were required for the development of CD8 α IELs compared to those required for negative selection. We also showed that IL-15 has an inhibitory effect on negative selection, and that both IL-2 and IL-15 promote the maturation and expansion of CD8 α IEL precursors. Consistent with a previous report³³, agonist peptide presentation by both hematopoietic and non-hematopoietic cells could support CD8 α IEL development in this system. However, hematopoietic cells were uniquely required to drive later stages of maturation, marked by T-bet induction and proliferation. We also observed that agonist selection was accompanied by elevated intracellular calcium and a confined migration pattern. Our results define key factors that determine whether self-reactive T cells undergo negative selection or adopt the CD8 α IEL fate in the thymus.

RESULTS

A proportion of self-reactive thymocytes do not undergo negative selection

To study factors that influence thymocyte fate following antigen encounter, we employed a thymic tissue slice system in which thymocytes of defined specificity are overlaid onto vibratome-cut thymic slices, after which they migrate into the slice and undergo a relatively synchronous wave of development^{22,23,25–27}. In this study, we used thymocytes from OT-I TCR transgenic mice and exposed them to agonist peptide derived from chicken ovalbumin (SIINFEKL, OVA_p) by adding OVA_p directly to tissue slices from wild type (WT) mice, or by using thymic slices from RIPmOVA transgenic mice, in which ovalbumin is expressed by a subset of medullary thymic epithelial cells. We evaluated the efficiency of negative selection in this system by including a reference population bearing an irrelevant TCR (F5 TCR transgenic or wild type thymocytes), and quantified thymocyte death as the ratio of live OT-I:reference thymocytes remaining in the slice. Consistent with previous studies^{23,27,28}, we observed a significant loss of OT-I thymocytes on both RIPmOVA slices and slices to which OVA_p had been added, as well as a large proportion of viable OT-I thymocytes that remained in the slice after 16 h of culture (Fig. 1a). The majority of surviving OT-I thymocytes expressed high levels of CD69, indicating that the surviving thymocytes had encountered antigen and experienced strong TCR signals (Fig. 1b).

Previous studies of the in situ behavior of autoreactive thymocytes have revealed migratory arrest and calcium flux following addition of agonist peptide^{22,23}. On the other hand, continued migration within confinement zones was reported in a steady state model of AIRE-dependent negative selection²⁴. To further explore the behavior of auto-reactive thymocytes undergoing death or survival, we performed 2-photon time-lapse imaging of OT-I thymocytes within RIPmOVA thymic slices. We first depleted OT-I thymocytes of the most mature CD8 single positive cells (CD8SP) (Supplementary Fig. S1). We then labeled thymocytes with a fluorescent ratiometric calcium indicator dye and allowed them to migrate into RIPmOVA thymic slices, and performed 2-photon time-lapse imaging after 3–7 h of culture. The majority of OT-I thymocytes localized to the medullary region of thymic tissue slices (ref²³ and data not shown), as expected given that both post-selection DP thymocytes and the remaining semi-mature CD8 SP thymocytes express a medullary chemokine receptor pattern (CXCR4⁺CCR7⁺)²⁵. On average, OT-I thymocytes in RIPmOVA slices displayed higher intracellular calcium levels (average corrected calcium ratio of 0.2 versus 0.0, Fig. 1c) and lower speed (6.0 versus 10 μ m/min, Fig. 1c) compared to thymocytes on wild type (no OVA) slices. Interestingly, we observed two distinct behaviors amongst thymocytes on RIPmOVA slices: a population with low speed and high calcium levels (483/757, 64% of total tracks), and a population with more rapid migration (Fig. 1c). In contrast, the majority of tracks on slices without OVA exhibited rapid migration, with only 20/188 tracks (11%) exhibiting low speed and high calcium levels (Fig. 1c). Notably, even the rapidly migrating (>9 μ m/min) thymocytes in RIPmOVA slices displayed slightly higher intracellular calcium compared to those in wild type (no OVA) slices (0.1 versus 0.0 average corrected calcium ratio, Fig. 1c, d). Moreover, the rapidly migrating OT-I thymocytes in RIPmOVA slices also displayed a lower directionality index, and reduced displacement from origin of migration (Fig. 1e, f) indicative of a more confined pattern of migration. In addition, visual inspection of tracks of OT-I thymocytes in RIPmOVA slices revealed multiple examples in which two or more confined tracks occupied the same 3-dimensional space, in close proximity to DC and AIRE-expressing mTECs (Supplementary Movies 1 and 2). Thus, thymocytes can make two distinct responses to encounter with agonist ligands: either migratory arrest with high intracellular calcium, or rapid, confined migration with slightly elevated calcium.

Thymocytes that survive negative selection are TCR α β CD8 α intraepithelial lymphocyte precursors

To determine whether the thymocytes that survived negative selection represented CD8 α IEL precursors, we investigated the phenotype of surviving OT-I thymocytes from thymic slices containing OVA. We depleted OT-I thymocytes of the most mature CD8SP (Supplementary Fig. S1), and overlaid the remainder onto WT thymic slices with OVA_p, or RIPmOVA slices, harvested at 96 h, and analyzed by flow cytometry. OT-I thymocytes that survived negative selection proliferated within the slice and expressed markers associated with a CD8 α IEL precursor phenotype, including CD122, PD-1, T-bet, and the gut homing marker $\alpha_4\beta_7$ integrin^{2,3,5,8,17} (Fig. 2a). In addition, OT-I thymocytes that had been exposed to OVA downregulated CD8 β relative to CD8 α , implying higher expression of the CD8 α form of the co-receptor (Fig. 2a).

To determine the kinetics with which thymocytes undergo these phenotypic changes, we performed a time course in which thymic slices treated with OVA_p were harvested after 1–4 days in culture. We observed that thymocytes exposed to OVA_p exhibited decreased expression of both CD8 β and CD8 α at day 1 (Fig. 2b), in line with studies demonstrating double-positive (DP) “dulling”, or the downregulation of both CD4 and CD8, in response to antigen stimulation^{2,5,34}. While CD8 β expression remained low thereafter,



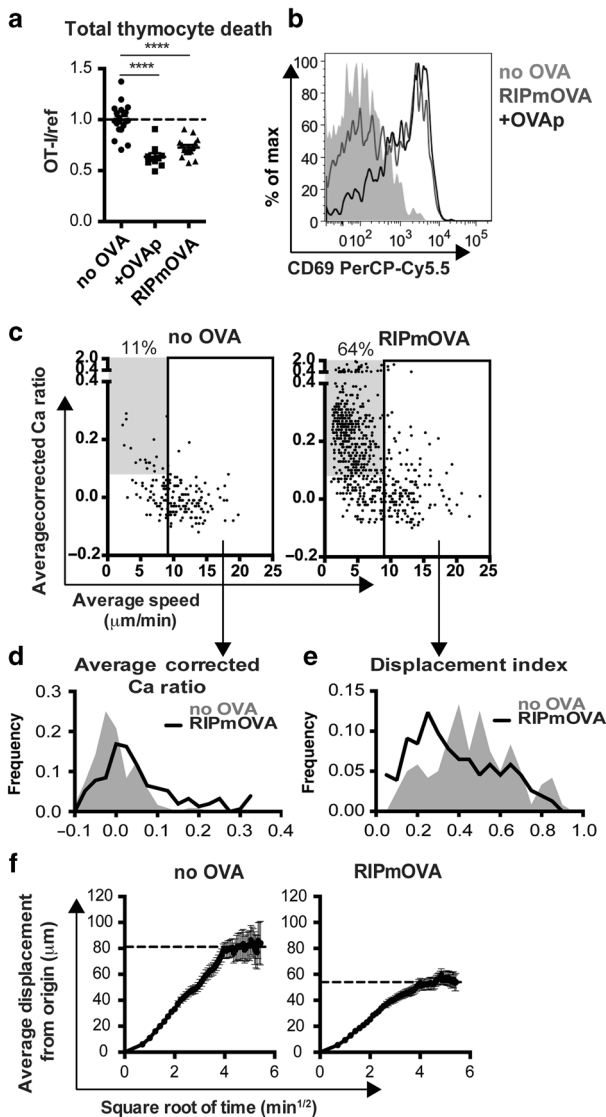


Fig. 1 A proportion of OT-I thymocytes survive negative selection, and exhibit confined migration. **a, b** Total OT-I thymocytes were overlaid onto the indicated thymic slices with reference thymocytes, and slices were harvested after 16 h for flow cytometric analysis. **a** Negative selection displayed as the ratio of live OT-I thymocytes relative to live reference thymocytes, normalized to no OVA controls. **b** CD69 expression on gated OT-I thymocytes. Data are representative of **b** or pooled from **a** 4 independent experiments, with mean and SEM of $n = 19\text{--}20$ thymic slices, where each dot represents an individual slice. **** $p < 0.0001$ (one-way ANOVA with Bonferroni's correction). **c–f** OT-I thymocytes were depleted of mature CD8 single positives (Supplementary Fig. S1) and labeled with the fluorescent ratiometric calcium indicator dye Indo-1 LR prior to overlay on WT or RIPmOVA thymic slices. Thymocytes were allowed to migrate into slices for 2 h, then imaged by two-photon microscopy 0–7 h later. Data are pooled from 4 (RIPmOVA) or 2 (WT) imaging runs. **c** Average speed versus relative calcium (calculated as described in Materials and Methods) where each dot represents an individual thymocyte track (RIPmOVA, $n = 757$; WT, $n = 188$). Numbers indicate the % of tracked thymocytes with low speed and high calcium tracks (gray box: average speed $< 9 \mu\text{m}/\text{min}$ and average corrected calcium > 0.08). Solid rectangle represents cutoff for fast tracks (average speed $> 9 \mu\text{m}/\text{min}$) used for the plots shown in **d–f**. **(d–e)** Average corrected calcium ratio **(d)** and displacement index **(e)** of fast ($> 9 \mu\text{m}/\text{min}$) tracks, where $n = 154$ (RIPmOVA) or 120 (WT) tracks. **f** Average displacement versus the square root of time for fast ($> 9 \mu\text{m}/\text{min}$) tracks on WT or RIPmOVA thymic slices. Black dotted lines indicate estimated plateau of confined migration, and error bars indicate SEM.

expression of CD8 α increased by day 2, resulting in a decreased CD8 β to CD8 α ratio (Fig. 2c). We also observed that thymocytes exposed to OVAp exhibited a slight upregulation of PD-1 as early as day 1, with PD-1 expression becoming maximal at day 2 and remaining elevated above baseline thereafter (Fig. 2d). In contrast, increases in CD122 and T-bet expression first became apparent at day 2 of culture and increased steadily thereafter (Fig. 2d). Finally, we noted that the majority of proliferation occurred between 2 and 3 days of culture (Fig. 2e).

As an additional indication of the timing of phenotypic changes accompanying IEL development, we also examined the relationship between cell division and marker expression at day 2 of culture (Supplementary Fig. S2a). Consistent with time course data, OT-I thymocytes upregulated PD-1 prior to cell division, whereas CD122 or T-bet upregulation was only observed on divided cells (Supplementary Fig. S2b, c). Furthermore, CD122 and T-bet expression were first detectable at division 1 and 2, respectively, suggesting that CD122 expression precedes T-bet expression (Supplementary Fig. S2b, c). In addition, OT-I thymocytes retained low expression of CD8 β but increased expression of CD8 α as they proliferated (Supplementary Fig. S2d). These data indicate that a decrease in the CD8 β/α ratio and upregulation of PD-1 begin very early after antigen encounter, followed by initiation of proliferation and increases in CD122, and finally T-bet expression.

To confirm that OT-I thymocytes that escaped negative selection were distinct from conventional activated T cells, we compared OT-I thymocytes to lymph node OT-I T cells after culture on thymic slices with or without OVAp. Both OT-I thymocytes and OT-I T cells proliferated extensively in OVA-containing slices, and had similar expression of CD122, PD-1, and T-bet (data not shown). However, whereas OT-I thymocytes exposed to antigen expressed lower levels of CD8 β relative to CD8 α , the relative expression of CD8 β versus CD8 α in OT-I T cells was unaffected by antigen exposure (Fig. 2f). In addition, OT-I thymocytes that developed in the presence of OVA exhibited more robust production of IFN γ in response to restimulation by OVA-loaded DC (Fig. 2g), a characteristic previously described for CD8 α IELs^{35–37}. These observations indicate that OT-I thymocytes that survive negative selection are distinct from conventional activated CD8 T cells, and instead resemble CD8 α IELs.

To investigate whether OT-I thymocytes that survive negative selection represent bona fide CD8 α IEL precursors, we examined their ability to give rise to CD8 α IEL in vivo. We cultured allelically marked (CD45.1) OT-I thymocytes on thymic slices with or without OVAp for 96 h, then dissociated the slices and transferred thymocytes into Rag2^{-/-} hosts (Fig. 3a). One week after transfer, OT-I T cells, along with slice resident cells (CD45.2), could be detected in the intraepithelial lymphocyte compartment of the small intestine (Fig. 3b). The percentage of OT-I thymocytes was reduced when donor populations came from cultures containing OVAp (Fig. 3b), consistent with negative selection observed in these cultures (Fig. 1a). Moreover, OT-I thymocytes that had been exposed to OVAp during thymic slice culture gave rise to a substantial population of CD8 α ⁺CD8 β ⁻ IELs, whereas this population was minimal among cells that had not been exposed to OVAp (Fig. 3c). Even amongst OT-I cells that retained some CD8 β expression, the levels of CD8 β relative to CD8 α was lower amongst OT-I IELs that had not been exposed to OVA during development (Fig. 3c). Taken together, these data demonstrate that OT-I thymocytes that survive negative selection in thymic tissue slices can home to the gut and give rise to CD8 α IEL.

Higher affinity threshold for CD8 α IEL development compared to negative selection

Since both negative selection and agonist selection into the CD8 α IEL lineage occur within the thymic slice, this provides a useful experimental system for investigating factors that influence these alternative fates. Negative selection and CD8 α IEL

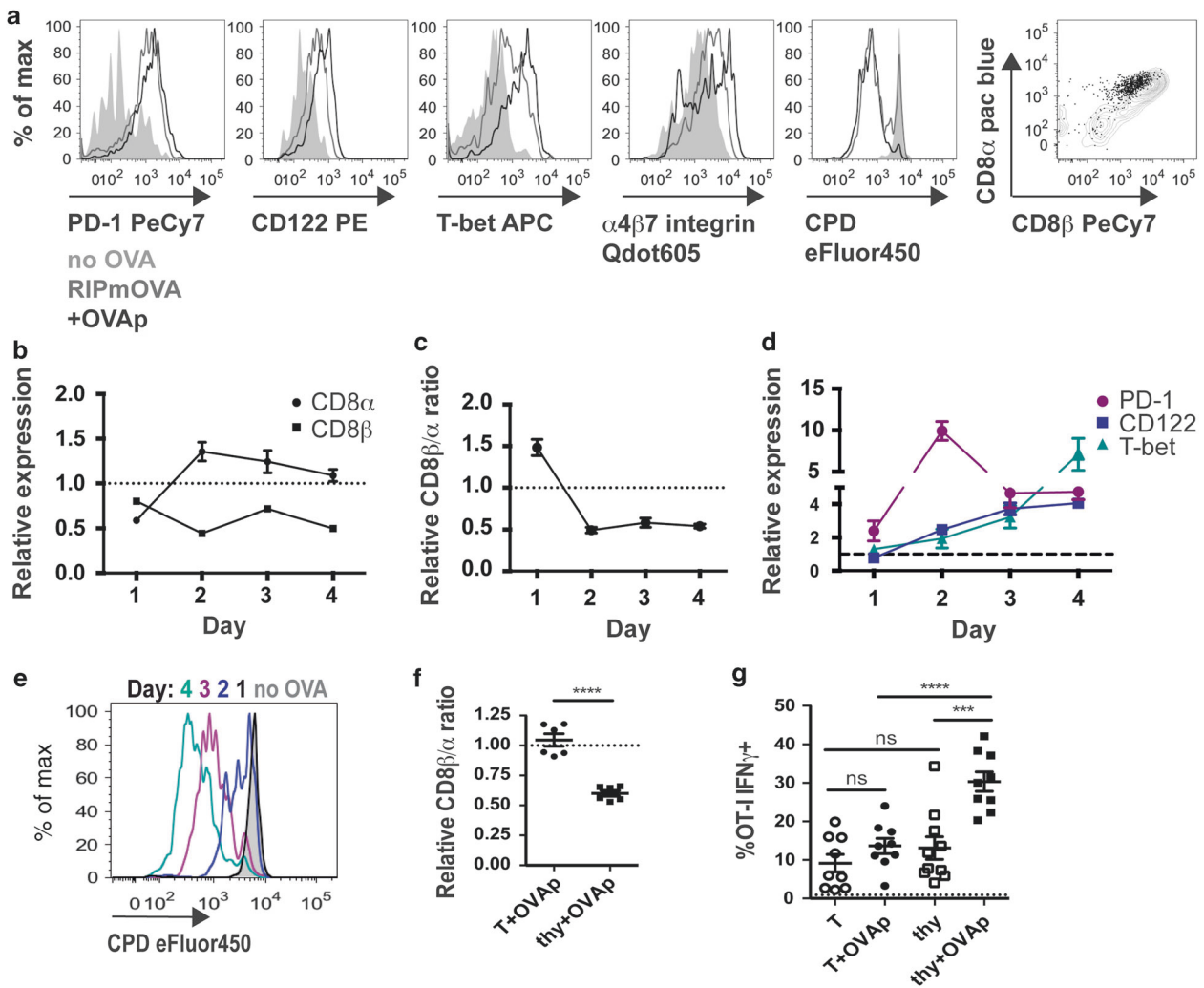


Fig. 2 Thymocytes that survive negative selection develop a CD8 α IEL precursor phenotype. **a–e** OT-I thymocytes were depleted of the most mature CD8 single positives and stained with cell proliferation dye eFluor450 (CPD450) prior to overlay onto the indicated thymic slices, which were harvested for flow cytometric analysis 1–4 days later. Data are representative of 2 independent experiments. **a** Representative flow cytometry plots of CD122, T-bet, PD-1, α 4 β 7 integrin, CPD450, and CD8 α versus CD8 β expression in gated OT-I thymocytes cultured on RIPmOVA thymic slices, or WT thymic slices with or without OVAp for 4 days. Gray histograms and dots represent OT-I on slices without OVA, black lines and dots represent OT-I on slices with OVAp, and dark gray lines represent OT-I on RIPmOVA slices. **b** Expression of CD8 α and CD8 β by OT-I thymocytes cultured on WT thymic slices with OVAp for the indicated times, displayed as the ratio of the Mean Fluorescence Intensity (MFI) of sample relative to no OVA control slices. **c** Relative CD8 β / α ratio of OT-I thymocytes on WT thymic slices with OVAp over time, displayed as the ratio of the MFI of CD8 β MFI/CD8 α MFI, normalized to no OVA control slices. **d** Expression of T-bet, CD122, and PD-1 expression over time in thymocytes on WT slices with OVAp, displayed as the ratio of the MFI of the indicated marker relative to no OVA control slices. Data are compiled from two independent experiments, with mean and SEM shown. **e** Representative flow cytometry plot displaying dilution of CPD450 in OT-I thymocytes on slices with OVAp after the indicated days of culture. **f, g** OT-I thymocytes depleted of the most mature CD8 single positives or OT-I T cells collected from the lymph nodes were overlaid onto thymic slices to which OVAp was added, and analyzed 96 h later. **f** Fold change in CD8 β / α ratio of OT-I thymocytes (thy) or T cells (T) after 96 h on thymic slices, displayed as the ratio of CD8 β MFI/CD8 α MFI relative to no OVA samples, where each dot represents an individual slice. Data are compiled from 2 independent experiments. **g** Production of IFN γ by OT-I thymocytes (thy) or OT-I T cells (T) after restimulation with OVA-loaded DC, displayed as percent of IFN γ + OT-I. Dashed line represents the average percent of IFN γ + cells in culture with unloaded DC. Data are pooled from 3 independent experiments, with mean and SEM of $n = 9$ thymic slices, where each dot represents an individual slice. ns not significant ($p > 0.05$), **** $p < 0.0001$ (one-way ANOVA with Bonferroni's correction).

development both require strong TCR signals compared to positive selection, but whether the TCR affinity threshold for CD8 α IEL development is higher or lower than that for negative selection remained unclear. To investigate this question, we added high affinity, SIINFELK OVA peptide (OVAp), or a peptide variant with lower affinity for the OT-I TCR (Q4p)³⁸ to thymic slices and determined the extent of negative selection and agonist selection in response to each peptide. Q4p was able to induce negative selection and stimulated CD69 upregulation on the majority of surviving thymocytes (Fig. 4a, b). However, thymocytes exposed to

Q4p failed to upregulate T-bet, CD122, and PD-1, and did not have the relative decrease in the ratio of CD8 β to CD8 α observed in response to OVAp (Fig. 4c–f). Thus, although both OVAp and Q4p were able to induce negative selection, only the highest affinity OVA peptide was able to induce a CD8 α IEL precursor phenotype.

IL-15 prevents negative selection while both IL-15 and IL-2 promote CD8 α IELp maturation
 Thymic precursors of CD8 α IEL have previously been shown to express CD122, a shared subunit of the IL-15 and IL-2

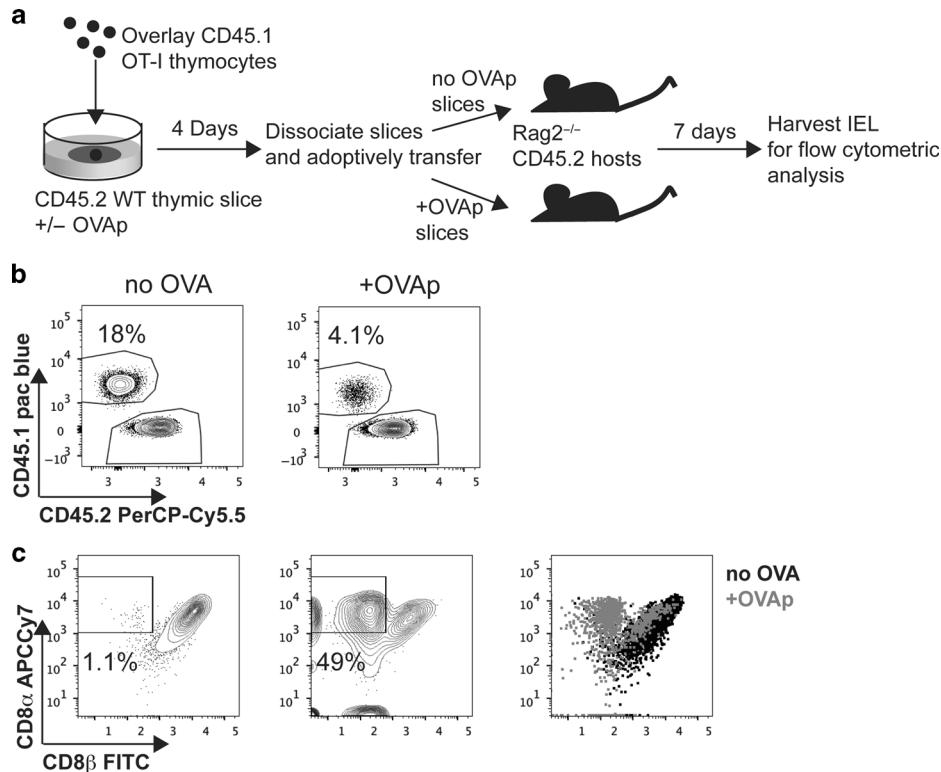


Fig. 3 Thymocytes that survive negative selection can home to the intestinal epithelium and give rise to CD8 α IELs. **a** Schematic of experimental setup: OT-I thymocytes depleted of mature CD8 single positives were overlaid onto thymic slices that were treated with OVAp. After 96 h, thymic slices were dissociated and adoptively transferred into Rag2^{-/-} mice. 1 week post-transfer, intraepithelial lymphocytes (IELs) were harvested from the small intestine. **b** Representative flow plots depicting gated TCR β ⁺ IELs, showing the proportion derived from OT-I thymocytes versus slice resident thymocytes, based on CD45.1/CD45.2 congenic markers. **c** Representative flow plots depicting expression of CD8 α versus CD8 β in OT-I IELs. Gates show proportion of OT-I thymocytes that are CD8 β ⁻. Data are representative of 2 independent experiments, with $n = 2-4$ mice per condition in each experiment.

receptors^{3,17,21}. Interestingly, OT-I thymocytes exposed to OVAp in thymic slice culture also upregulated CD25, the high-affinity α -chain of the IL-2 receptor (Supplementary Fig. S3a). Moreover, we found that CD25 is expressed by approximately 4% of endogenous CD8 α IEL precursors (Supplementary Fig. S3b), suggesting potential roles for both IL-15 and IL-2 in their development. To further examine the roles of IL-15 and IL-2 in CD8 α IEL development, we added exogenous IL-15 or IL-2 to thymic slices containing OT-I thymocytes and OVAp, and investigated the effect on negative selection and CD8 α IEL development. To supply IL-15, we used IL-15/IL-15 α complexes (IL-15c) to mimic trans-presentation of IL-15 bound to the IL-15 α ³⁹⁻⁴¹. To supply IL-2, we used complexes of IL-2 and antibody specific for IL-2 (IL-2c), which have greater biological activity compared to IL-2 alone⁴². To assess effects on negative selection, we overlaid OT-I and reference thymocytes onto thymic slices followed by treatment with OVAp with and without added cytokines. We observed that IL-15, but not IL-2, decreased negative selection, as indicated by an increase in the OT-I:reference ratio at 16 h (Fig. 5a). This increase was not due to IL-15-induced proliferation, because OT-I thymocytes had not proliferated at this time point under any of the conditions (Fig. 5a, data not shown). These data suggest that IL-15, but not IL-2, might promote the CD8 α IEL fate by limiting the death of self-reactive thymocytes, which might allow a larger proportion to develop into CD8 α IEL precursors.

We also observed that treatment with both exogenous IL-15 and IL-2 resulted in a marked decrease in the ratio of CD8 β to CD8 α at 48 h, as well as an increase in T-bet expression, which was more pronounced in response to IL-2 (Fig. 5b, c). In addition, both IL-15 and IL-2 resulted in a robust increase in the frequency of OT-I thymocytes present in the slice at 96 h (Fig. 5d). To test whether a

lack of IL-2 and IL-15 signals might impact CD8 α IEL precursor development, we overlaid OT-I thymocytes and OVAp onto either IL-2^{-/-} thymic slices, or IL-15 α ^{-/-} thymic slices, in which IL-15 signaling is deficient due to a lack of trans-presentation^{40,41}. We observed a modest reduction in T-bet expression in both environments (Fig. 5e, f), consistent with previous reports that mice deficient in IL-15 have a reduction in T-bet^{hi} CD8 α IEL precursors in the thymus^{3,8}. Taken together, these data suggest that both IL-15 and IL-2 can promote the CD8 α IEL precursor maturation and expand the CD8 α IEL precursor population.

Peptide presentation by hematopoietic cells promotes the maturation and expansion of CD8 α IEL precursors. The thymus contains a variety of peptide-presenting cells, but which cells can serve as antigen presenting cells for CD8 α IEL development remained unclear. To address this question, we made use of Kbm1 mice, which carry an allelic version of the MHC class I K gene that is unable to stimulate OT-I T cells⁴³. To restrict antigen presentation to hematopoietic cells (including DCs and macrophages), we transferred WT bone marrow into Kbm1 hosts (referred to as WT \rightarrow Kbm1 mice). Reciprocally, we transferred Kbm1 bone marrow into WT hosts to restrict antigen presentation to stromal cells (including epithelial cells) (referred to as Kbm1 \rightarrow WT mice). We then compared the efficiency of CD8 α IEL development of OT-I thymocytes overlaid onto thymic slices from chimeric mice and treated with OVAp. We observed a modest reduction in the percent of OT-I thymocytes that expressed high levels of CD122 and PD-1 at 48 h in both WT \rightarrow Kbm1 and Kbm1 \rightarrow WT thymic slices, suggesting that both stromal and hematopoietic compartments contribute to the development of IEL precursors (Fig. 6a), consistent with a previous study³³.

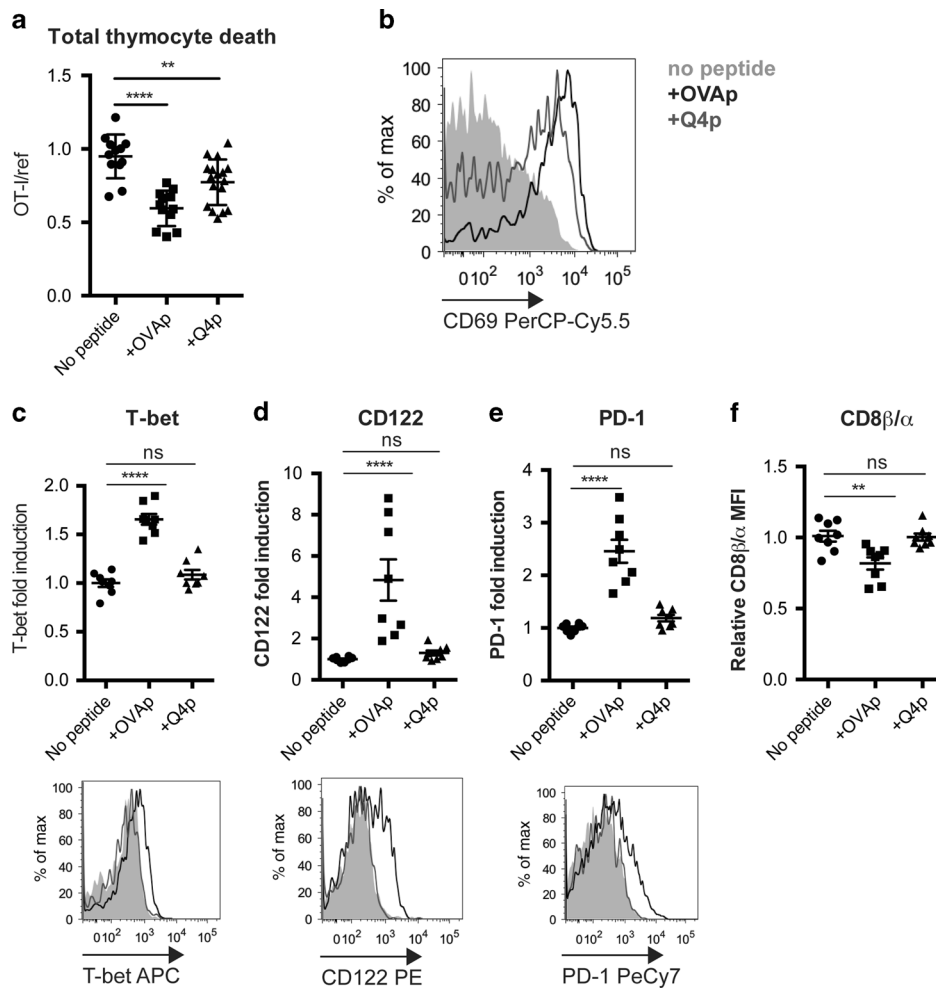


Fig. 4 Only very high affinity agonists drive CD8 α IEL development. OT-I thymocytes depleted of mature CD8 single positives were overlaid onto WT thymic slices to which OVAp (SIINFEKL) or lower-affinity Q4 peptide was added. In some cases (**a**, **b**) a reference population was added with the OT-I thymocytes. Slices were harvested at 16 (**a**, **b**) or 96 (**c–f**) hours for flow cytometric analysis. **a** Negative selection displayed as the ratio of live OT-I thymocytes relative to live reference thymocytes, normalized to no OVA controls. **b** Antigen recognition of OT-I thymocytes displayed as expression of the activation marker CD69. Data are representative of **b** or pooled from (**a**) 3 independent experiments, with mean and SEM of $n = 11–15$ total slices per condition, where each dot represents an individual slice. **c–e** Expression of T-bet (**c**), CD122 (**d**), or PD-1 (**e**) in OT-I thymocytes presented as fold induction displayed as MFI relative to levels in no peptide controls (top), or representative flow cytometry plots (bottom). **f** Fold change in CD8 β/α ratio displayed as the ratio of CD8 α MFI/CD8 β MFI relative to no peptide samples, where each dot represents an individual slice. Data are representative of (bottom panels) or pooled from (top panels) 2 independent experiments, with mean and SEM of $n = 6$ total slices per condition, where each dot represents an individual slice. ns not significant ($p > 0.05$), ** $p < 0.01$, **** $p < 0.0001$ (one-way ANOVA with Bonferroni’s correction).

Interestingly, thymocytes that encountered antigen on hematopoietic cells proliferated more extensively (slices from WT \rightarrow Kbm1 and WT \rightarrow WT) than thymocytes that encountered antigen only on stromal cells (Kbm1 \rightarrow WT slices) (Fig. 6b). In contrast, upregulation of T-bet was significantly abrogated when hematopoietic cells could not present OVA (in Kbm1 \rightarrow WT slices), while restricting antigen presentation to hematopoietic cells resulted in an increase in T-bet expression (in WT \rightarrow Kbm1 slices) (Fig. 6c). Taken together, these data suggest that while peptide presentation by stromal cells can promote the initial differentiation of CD8 α IEL precursors, peptide presentation by hematopoietic cells more efficiently supports their late maturation, including proliferation and T-bet upregulation.

DISCUSSION

Strong TCR signaling during thymic development can lead to either the removal of self-reactive cells by negative selection, or

their diversion into regulatory lineages, termed agonist selection. While this phenomenon has been extensively investigated for regulatory T cell development from MHC class II-restricted thymocytes, less is known about the agonist selection of CD8 α IEL. Here, we develop an experimental system in which thymocytes bearing an MHC class I-specific TCR undergo both negative selection and CD8 α IEL development after encounter with agonist peptide within thymic tissue slice culture, and we use this system to investigate factors that influence auto-reactive thymocyte fate. We found that higher affinity interactions are required to drive agonist selection of CD8 α IELs compared to that required for negative selection. We also found that both IL-2 and IL-15 can promote the maturation and expansion of CD8 α IEL precursors, while IL-15 has the additional effect of inhibiting negative selection. Finally, our data suggest that while peptide presentation by both stromal and hematopoietic cells can drive the initial development of CD8 α IELs, hematopoietic cells more efficiently drives their expansion and further maturation. These

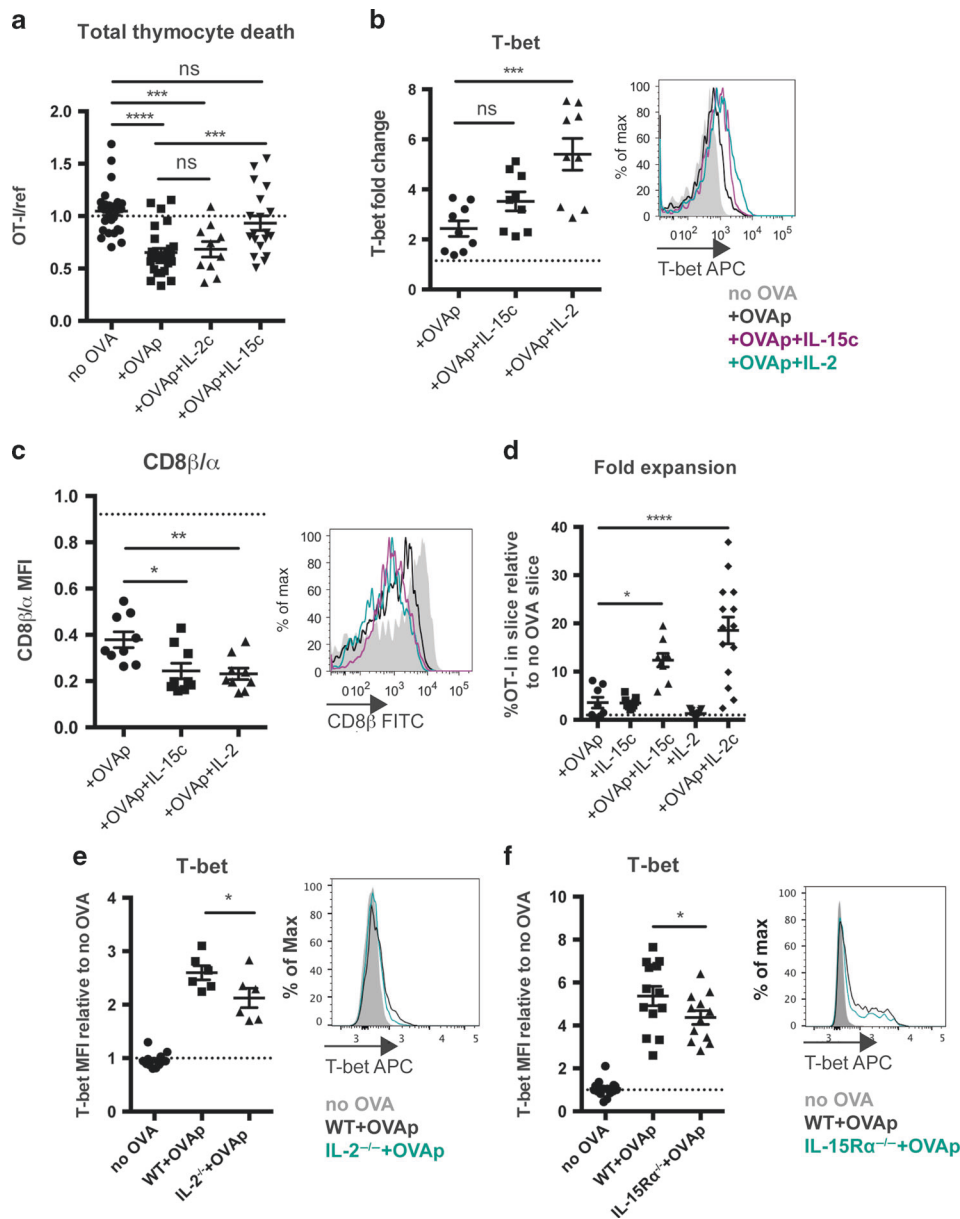


Fig. 5 Distinct effects of IL-15 and IL-2 on survival, maturation, and expansion of CD8 $\alpha\alpha$ IEL precursors. Total OT-I thymocytes (a) or OT-I thymocytes depleted of mature CD8 single positives (b–d) were overlaid onto thymic slices to which OVAp was added, followed by treatment with IL-15R α /IL-15 complexes or IL-2 α -IL-2 antibody complexes. Slices were harvested at 16 (a), 48 (b, c), or 96 (d) hours for flow cytometric analysis. a Negative selection displayed as the ratio of live OT-I thymocytes relative to live reference thymocytes, normalized to no OVA controls. Data are pooled from 3 independent experiments, with mean and SEM of $n = 13$ –19 total slices per condition, where each dot represents an individual slice. b Changes in CD8 β expression displayed as the ratio of CD8 β MFI/CD8 α MFI relative to no OVA control samples (left) or representative flow cytometry depicting expression of CD8 β (right). Dashed line indicates the average CD8 β /CD8 α ratio in no OVA control samples across all treatment conditions; no significant differences in the CD8 β /CD8 α ratio were observed in response to cytokine treatment without OVAp. c Expression of T-bet in OT-I thymocytes presented as representative flow cytometry (right), or fold induction of T-bet displayed as MFI relative to no OVA control samples (left). Dashed line indicates the average T-bet expression in no OVA control samples across all treatment conditions; no significant differences in T-bet expression were observed in response to cytokine treatment without OVAp. Data are representative of (right panels of b,c), or pooled from (left panels of b, c) 3 independent experiments, with mean and SEM of $n = 9$ total slices per condition, where each dot represents an individual slice. d Fold expansion of OT-I thymocytes at 96 h, displayed as percent of the total slice made up of OT-I thymocytes relative to untreated, no OVA control slices. Data are pooled from 4 independent experiments, with mean and SEM of 15–16 total slices per condition, where each dot represents an individual slice. e, f OT-I thymocytes depleted of mature CD8 single positives were overlaid onto WT, and IL-2 $^{-/-}$ (e), or IL-15R $\alpha^{-/-}$ (f) thymic slices to which OVAp was added, and slices were harvested 48 h later for flow cytometric analysis. Expression of T-bet in OT-I thymocytes presented as representative flow cytometry (right), or fold induction of T-bet displayed as MFI relative to no OVA control samples (left). Dashed line indicates the average T-bet expression in no OVA control samples across all thymic slices; no significant differences in T-bet expression were observed between WT and IL-2 $^{-/-}$ (e) or IL-15R $\alpha^{-/-}$ thymic slices without OVAp. Data are representative of (right panels of e, f), or pooled from (left panels of e, f) 2 (e), or 3 (f) independent experiments, with mean and SEM of $n = 6$ –12 total slices per condition, where each dot represents an individual slice. ns not significant ($p > 0.05$), * $p < 0.05$, ** $p < 0.01$, *** $p < 0.001$, **** $p < 0.0001$ (one-way ANOVA with Bonferroni's correction).

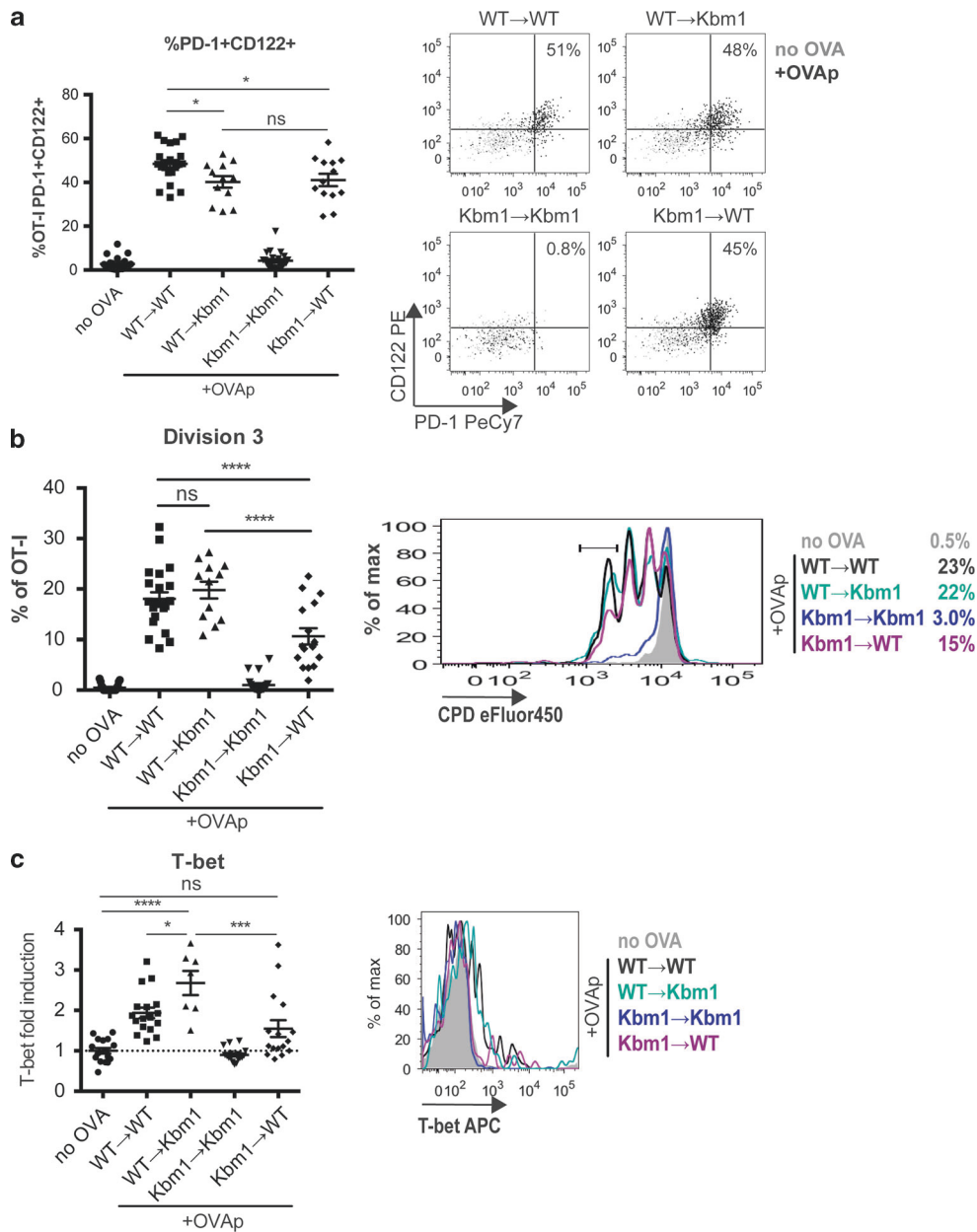


Fig. 6 Effects of peptide-presenting cell on the development of CD8 α IEL precursors. OT-I thymocytes depleted of mature CD8 single positives were stained with CPD450 and overlaid onto thymic slices from WT→Kbm1, Kbm1→WT, WT→WT, or Kbm1→Kbm1 bone marrow chimeric mice. In some experiments, WT or Kbm1 mice were used instead of WT→WT or Kbm1→Kbm1 control chimeras, respectively, with equivalent results. OVAp was added to thymic slices, which were harvested 48 h later for flow cytometric analysis. **a** Percent of OT-I thymocytes expressing CD122 and PD-1, displayed as values (left) or representative flow cytometry plots (right). **b** Expression of T-bet in OT-I thymocytes exposed to OVAp presented as Mean Fluorescence Intensity (MFI) of T-bet relative to no OVA controls (left), or representative flow cytometry plot (right). Dashed line indicates the average T-bet expression in no OVA control samples across all treatment conditions. **c** Proliferation of OT-I thymocytes displayed as percent of OT-I thymocytes that have undergone 3 cellular divisions, determined based on dilution of CPD450 according to the gate shown in the representative flow cytometry plot (right). Data are pooled from (left panels) or representative of (right panels) 3 (WT→Kbm1 and Kbm1→WT conditions) or 5 (no OVA, WT→WT, Kbm1→Kbm1 conditions) experiments with mean and SEM of $n = 12$ –22 total slices, where each dot represents an individual slice. ns not significant ($p > 0.05$), * $p < 0.05$, *** $p < 0.001$, **** $p < 0.0001$ (one-way ANOVA with Bonferroni's correction).

findings identify factors that support CD8 α IEL development (Supplementary Fig. S4), and highlight the importance of the thymic environment and peptide-presenting cell, along with TCR affinity for self-ligands, in shaping T cell fate.

By definition, agonist selection requires stronger TCR signals compared to positive selection, but the relative TCR signal strength required for agonist versus negative selection is less clear. For class II restricted T cells, recent studies indicate that a

broad range of self-reactivity can lead to regulatory T cell development, resulting in a tT_{reg} TCR repertoire that overlaps extensively with both conventional CD4 T cells and thymocytes undergoing negative selection^{9,44}. In contrast, we find that CD8 α IEL development requires stronger TCR signals compared to negative selection, since a peptide with moderately high affinity for the TCR was capable of inducing negative selection, but not CD8 α IEL development. The notion that stronger TCR signals are

required to drive CD8 α IEL development compared to negative selection is also consistent with the lack of overlap between the CD8 α IEL and conventional CD8 TCR repertoires^{2,5} (Supplementary Fig. S4a). The less stringent avidity requirements for the development of tT_{regs} compared to CD8 α IEL may relate to the greater impact of cell death in thymic selection of class I versus class II restricted T cells⁴⁵, and the relatively modest role of deletion in maintaining tolerance within CD4 lineage T cells due to the diversion of moderately self-reactive CD4 T cells into the regulatory T cell lineage^{46,47}. These findings might also help to explain the observation that class I-restricted T cells with moderate affinity for self are the primary mediators of autoimmunity⁴⁸, since such thymocytes are more likely to escape negative selection, but less likely to undergo agonist selection, compared to thymocytes with higher affinity for self (Supplementary Fig. S4c).

Taking advantage of the synchronicity of development in the thymic slice model, we define the kinetics of phenotypic changes in thymocytes undergoing CD8 α IEL development, revealing an initial transient upregulation of PD-1 at 1 day and the induction of T-bet and proliferation at 3 days after agonist encounter. It is interesting to consider this phenotypic progression in light of current information about heterogeneity amongst thymic IEL precursors. A recent study identified PD1⁺T-bet⁻ and PD-1⁻Tbet⁺ populations, and provided evidence that these correspond to distinct lineages, both of which can contribute to the mature IEL compartment³. Other studies have proposed a precursor-product relationship between T-bet⁻ and T-bet⁺ precursors, based on the more mature phenotype of T-bet⁺ IELp, as well evidence that in vitro exposure to IL-15 can induce T-bet upregulation in IELp^{3,8,17,21,33}. Importantly, these two possibilities are not mutually exclusive. Indeed, our data, together with previous reports, suggest that the PD-1⁺Tbet⁻ compartment may be heterogeneous, with some cells being competent to leave the thymus and seed the intestinal compartment, and others destined to remain in the thymus and undergo further maturation into PD-1⁻ Tbet⁺ IELp.

IL-15 plays a crucial role for CD8 α IEL in the intestine, but its role in the thymic development of CD8 α IEL precursors has not been fully resolved. IL-15^{-/-} mice have normal numbers of total CD8 α IEL precursors, but lack a subset of the most mature T-bet⁺ CD8 α IEL precursors^{3,8,21}. Here, we show that IL-15, as well as the related common gamma chain cytokine IL-2, can drive multiple aspects of CD8 α IEL development, including proliferation, CD8 β downregulation, and T-bet upregulation. In addition, T-bet upregulation was impaired in the absence of IL-2 or IL-15 signaling, suggesting that these cytokines are needed to support later stages of CD8 α IEL precursor maturation. The modest effects of IL-2 and IL-15 deficiency on T-bet upregulation may suggest functional redundancy between these cytokines with regards to their role in CD8 α IEL precursor maturation, but we found that IL-15, but not IL-2, can inhibit negative selection, suggesting that IL-15 signals might promote the CD8 α IEL fate both by inhibiting negative selection and by actively promoting the CD8 α IEL developmental program (Supplementary Fig. 4b). Interestingly, there is evidence that IL-2 both prevents negative selection of tT_{regs}, and promotes their differentiation¹⁶. This could reflect a difference in the response of class I versus class II restricted thymocytes to IL-2, or a difference in the experimental systems used.

We have previously shown that distinct T cell fates are correlated with distinct patterns of thymocyte motility and TCR signaling^{22,23,25}. For example, positive selection is characterized by transient TCR signals interspersed with periods of active migration, whereas negative selection is characterized by sustained TCR signals and migratory arrest. Here, we observed that thymocytes in a synchronous model of exposure to a tissue-restricted antigen exhibited two distinct patterns of motility, correlating with their two distinct fates in this system. Some thymocytes exhibited behavior consistent with negative selection (high intensity TCR

signals and migratory arrest), whereas others displayed a distinctive motility behavior that might correlate with agonist selection. Specifically, these cells remained motile while exhibiting higher intracellular calcium levels and a more confined pattern of migration compared to thymocytes cultured without antigen. Given that PD-1 has been shown to inhibit TCR signaling-induced stop signals⁴⁹, it is tempting to speculate that the upregulation of PD-1 among CD8 α IELp might promote sustained motility despite receiving strong TCR signals, in contrast to the migratory arrest observed in thymocytes undergoing negative selection. We also observed examples of "confinement zones", in which the migration of multiple thymocytes appeared to be confined within the same 3-dimensional space. A similar pattern of confined migration was observed among thymocytes in the presence of a tissue-restricted antigen at steady-state²⁴. Thus, both the surviving thymocytes in a steady-state model of negative selection, and a portion of thymocytes in a synchronized model of negative selection, display a migration pattern suggestive of niches within the medulla that might support agonist selection.

Our observation that both peptide presentation by hematopoietic cells, as well as exogenous IL-2 and IL-15, enhanced certain aspects of the CD8 α IEL developmental program, suggest that thymic microenvironments enriched in these factors would support CD8 α IEL development. Medullary thymic epithelial cells (mTECs) are the major source of IL-15 in the thymus and closely associate with hematopoietic cells such as thymic DC^{30,50,51}. Thymic IL-2 derives from hematopoietic cells, particularly thymocytes⁵², and there is also evidence that spatial linkage of IL-2 with antigen presenting cells such as DC promotes tT_{reg} development^{10,26}. Thus, high-affinity TCR ligand provided by DCs, along with trans-presentation of IL-15 by neighboring mTECs and IL-2 production by mature thymocytes receiving strong TCR signals, together might provide specialized niches for agonist selection in the medulla. Previous studies also suggest that thymic microenvironments low for CD28 ligands would be expected to favor CD8 α IEL development over negative selection¹¹. Other cytokines, such as TGF β also contribute to CD8 α IEL development⁵³, and could also contribute to an agonist selection niche.

Altogether, our data suggest that a "niche" that efficiently supports CD8 α IEL development includes presentation of high affinity self-peptides by hematopoietic-derived cells together with IL-15 and/or IL-2, and support the idea that confined migration within such niches is a characteristic of agonist selection. These findings help to elucidate mechanisms by which divergent thymocyte fates are achieved from the same initial stimulus, and should inform future studies aimed at understanding the requirements for CD8 α IEL development in the thymus.

METHODS

Mice

All mice were maintained and bred in-house in an American Association of Laboratory Animal Care-approved facility at the University of California, Berkeley. All procedures were approved by the University of California, Berkeley Animal Use and Care Committee. C57BL/6, C57BL/6-Tg(Ins2-TFRC/OVA)296Wehi/WehiJ (RIPmOVA), B6(Cg)-Rag2tm1.1Cgn/J (Rag2^{-/-}), B6.C-H2-Kbm1/ByJ (Kbm1), B6.129P2-Il2tm1Hor/J (IL-2^{-/-}), and B6.SJL-Ptprca Pepcb/BoyJ (CD45.1) were from Jackson Labs. OT-I Rag2^{-/-} mice were from Taconic Farms. OT-I Rag2^{-/-} CD45.1 mice were generated by crossing OT-I Rag2^{-/-} mice to CD45.1 mice. F5 Rag1^{-/-} mice⁵⁴, CD11cYFP mice⁵⁵, and AireGFP mice⁵⁶ have been previously described. CD11cYFP RIPmOVA mice and AireGFP RIPmOVA mice were generated by crossing CD11cYFP or AireGFP mice to RIPmOVA mice, respectively. IL15R α ^{-/-} mice were generated by crossing B6.C-Tg(CMV-cre)1Cgn/J (Cmv-cre) mice with C57BL/6-Il15ratm2.1Ama/J (IL15R α flox/flox) mice, both from Jackson Labs. To generate bone marrow chimeras, bone marrow was collected

from the tibias and femurs of donor mice, then treated with ammonium chloride–potassium bicarbonate buffer to lyse red blood cells. Host mice were lethally irradiated (900rads) prior to intravenous injection of 5×10^6 bone marrow cells.

Thymocyte enrichment and labeling

Thymocytes were collected by dissociating whole thymic lobes through a 70 μ m cell strainer to obtain a cell suspension. For negative selection experiments, total OT-I and reference (B6 or F5 Rag1^{-/-}) thymocytes were stained with Cell Proliferation Dyes eFluor450 (1 μ M) or eFluor670 (0.5 μ M) (Thermo Fisher Scientific) at 10^7 cells/ml in PBS for 15 min at 37 °C prior to overlay on thymic slices. For all other experiments, OT-I thymocytes were depleted of mature CD8 single positives using anti-human/mouse β 7 integrin antibody (FIB504, Biolegend) and the EasySep Biotin Positive Selection Kit (Stemcell Technologies) according to product instructions. Following depletion, thymocytes were stained with CPD eFluor450 or eFluor670 as described above.

Thymic slices

Preparation of thymic slices has been previously described in detail⁵⁷. Briefly, thymic lobes were embedded in 4% agarose with low melting temperature (GTG-NuSieve Agarose, Lonza) before being sectioned into 200–400 μ m slices using a vibratome (1000 Plus sectioning system, Leica). Thymic slices were overlaid onto 0.4 μ m transwell inserts in 6 well tissue culture plates containing 1 ml of complete RPMI medium (containing 10% FBS, penicillin streptomycin, and 2-mercaptoethanol, cRPMI) under the transwell, and cultured at 37 °C. Ten microliters of cRPMI containing $0.5\text{--}2 \times 10^6$ thymocytes was overlaid onto each slice, and thymocytes were allowed to migrate into the slice for 2 h followed by the removal of excess thymocytes by gentle washing of the slice with PBS. Thymocytes actively migrate into the slices and localize properly within the tissue^{31,58}. Overlaid thymocytes were distinguished from slice-endogenous thymocytes using CD45.1/CD45.2 congenic markers, or in some cases, by staining with cell proliferation dyes. To introduce cognate antigen, 10 μ l of 1 μ M SIINFEKL (AnaSpec) or SIQFEKL (Q4, AnaSpec) in PBS was overlaid onto each slice for 30 min before excess was removed by pipetting. For IL-15 treatment, slices were overlaid with 50 ng recombinant IL-15/IL-15R α complex (Thermo Fisher) in 10 μ l of cRPMI following peptide treatment. To make IL-2 complexes, 1.5 μ g of recombinant IL-2 (Peprotech) and 7.5 μ g of functional grade anti-IL-2 antibody (JES6-1, Thermo Fisher) were incubated together at 37 °C for 30 min. Thymic slices were treated with 75 ng IL-2 (in complex) in 10 μ l PBS following peptide treatment.

Bone marrow-derived dendritic cell cultures and in vitro activation
Bone marrow was collected from the femurs and tibias of mice and resuspended in ammonium chloride–potassium bicarbonate buffer for lysis of red blood cells. Bone marrow cells were then plated at 10^6 cells/ml in cRPMI containing 20 ng/ml

granulocyte-macrophage colony-stimulating factor (GM-CSF, Peprotech), and cultured for 7 days. On day 6, media was replaced with fresh media containing GM-CSF. Semi-adherent cells were collected at day 7 and loaded with SIINFEKL in cRPMI containing 1 μ M peptide at 10^7 cells/ml for 30 min at 37 °C. BMDCs were then plated at 2×10^5 cells per well in 96 well U-bottom tissue culture plates and 3×10^5 thymocytes stained with 0.5 μ M eFluor670 (Thermo Fisher Scientific) were added per well. BMDCs and thymocytes were cultured together for 48 h prior to collection for flow cytometric analysis.

Adoptive transfers and isolation of intraepithelial lymphocytes

Thymic slices were collected at the indicated timepoints, dissociated, and filtered to remove agarose. 3×10^6 total cells were then injected intravenously into Rag2^{-/-} mice 4–7 weeks of age, and intraepithelial lymphocytes were collected from the small

intestine at 7 days post-transfer. The small intestine was harvested and cleaned of fat and connective tissue. Fecal contents were flushed out with PBS, and the tissue was cut into small pieces that were placed in 1 mM DTT in Hank's Balanced Salt Solution, and shaken at 37 °C for 1 h total, with collection of cells and replacement of new 1 mM DTT solution every 20 min. Samples were resuspended in 20% Percoll and overlaid onto 40% Percoll over 70% Percoll and spun. The 40/70 interface was collected and stained for flow cytometric analysis.

Flow cytometry

Single cell suspensions were resuspended in 24G2 supernatant containing the following antibodies: CD4 (GK1.5), CD8 α (53-6.7), CD8 β (H35-17.2), CD69 (H1.2F3), CD122 (Tm-b1), α 4 β 7 integrin (DATK32), PD-1 (29F.1A12), CD3 ϵ (145-2c11), TCR β (H57-597), CD45.1 (A20), CD45.2 (104), CD28 (37.51), on ice for 10 min. All antibodies were from Tonbo Biosciences, Thermo Fisher Scientific, or Biolegend. Cells were then washed in PBS and stained in Ghost Dye Violet 510 (Tonbo Biosciences) for 10 min on ice. To obtain single cell suspensions from thymic slices, slices were dissociated into FACS buffer (0.5% BSA in PBS) and filtered for removal of agarose before staining. For intracellular staining of IFN γ , cells were cultured with Protein Transport Inhibitor Cocktail for 4 h at 37 °C prior to staining. Following staining with cell surface antibodies and live/dead staining, cells were fixed using Cytofix/Cytoperm Kit (BD Pharmingen), then stained for IFN γ (XMGI.2). For intracellular staining of T-bet, cells were stained with cell surface antibodies and live/dead dye, then fixed and permeabilized using the FoxP3 Transcription Factor Staining Buffer Set (Thermo Fisher Scientific) according to the manufacturer's protocol prior to staining for T-bet (644814). All data was collected on a LSR II or BD Fortessa analyzer (BD Biosciences), and data were analyzed using FlowJo software (TreeStar).

Microscopy

For labeling, 10^7 thymocytes were incubated with 2 μ M Indo-1 LR (Teflabs) at 3×10^6 cells/ml for 90 min in cRPMI at 37 °C. For overlaying on thymic slices, the cell suspensions were adjusted to 5×10^5 cells/10 μ l and 10 μ l were gently overlaid onto thymic slices in transwells as described above. The cells were left to migrate into the slice for 2 h at 37 °C/5% CO₂, followed by gentle washing with PBS to remove the cells that failed to enter the slice. Thymic slices were prepared from RIPmOVA transgenic or non-transgenic mice. For some experiments RIPmOVA mice were crossed to AIRE-GFP or CD11cYFP reporter mice to allow for visualizing mTEC or dendritic cells, respectively. Thymic tissue slices were glued on coverglasses and medullary regions, identified by density of CD11cYFP or AIRE-GFP reporter⁺ cells, were imaged by two-photon laser scanning microscopy with a Zeiss 7 MP (Zeiss), while being perfused with warmed (37 °C), oxygenated phenol-free DMEM medium (GIBCO) at a rate 1 ml/min. Mode-locked Ti:sapphire laser Mai-Tai (Spectra-Physics) or Chameleon (Coherent) was tuned to 720 nm for Indo-1 LR excitation, or to 920 nm for CFP or GFP excitation, with appropriate filter sets. Imaging volumes of various sizes were scanned every 30 s for 20–60 min.

Image analysis

Imaris 7.3 (Bitplane) was used to determine cell positions over time and tracking. The x , y , and z coordinates as well the mean fluorescence intensities of the tracking spots for Ca²⁺-bound Indo-1 LR, Ca²⁺-free Indo-1 LR were exported. Motility parameters were calculated in MATLAB (Mathworks) with a custom code that is available upon request. Ca²⁺-ratio was calculated as a surrogate for Ca²⁺ intracellular concentration by dividing the mean fluorescence intensity of Ca²⁺-bound Indo-1 LR by the Ca²⁺-free Indo-1 LR. All the values were normalized so that the average Ca²⁺-ratio of migrating thymocytes in the no Ova control sample was zero (corrected Ca²⁺-ratio).



Statistics

Prism software (GraphPad) was used for all statistical analysis. P values of <0.05 were considered significant.

ACKNOWLEDGEMENTS

We thank members of the Robey lab for helpful discussion and technical advice, and H. Melichar for critical reading of the manuscript. We also thank O. Guevarra for technical assistance, P. Herzmark for assistance with two-photon imaging, and M. Anderson (UCSF) for providing AIRE-GFP reporter mice. This work was funded by NIH RO1AI064227 (E.A.R.), N.S.K. and B.M.W. were supported by NIH T32AI100829, and N. S.K. was supported by a University of California Cancer Research Coordinating Committee Fellowship.

AUTHOR CONTRIBUTIONS

N.S.K. designed and performed experiments, analyzed data and wrote the manuscript. A.H. designed and performed experiments and analyzed data. J.Y. performed experiments and analyzed data. B.M.W. designed and performed experiments. L.L. performed experiments. S.W.C. performed experiments. E.A.R. designed experiments, analyzed data and wrote the manuscript.

ADDITIONAL INFORMATION

The online version of this article (<https://doi.org/10.1038/s41385-020-0295-5>) contains supplementary material, which is available to authorized users.

Competing interests: The authors declare no competing interests.

Publisher's note Springer Nature remains neutral with regard to jurisdictional claims in published maps and institutional affiliations.

REFERENCES

1. Stritesky, G. L., Jameson, S. C. & Hogquist, K. A. Selection of self-reactive T cells in the thymus. *Annu. Rev. Immunol.* **30**, 95–114 (2012).
2. McDonald, B. D., Bunker, J. J., Ishizuka, I. E., Jabri, B. & Bendelac, A. Elevated T cell receptor signaling identifies a thymic precursor to the TCR $\alpha\beta$ +CD4 $^+$ CD8b $^-$ intraepithelial lymphocyte lineage. *Immunity* **41**, 219–229 (2014).
3. Ruscher, R., Kummer, R. L., Lee, Y. J., Jameson, S. C. & Hogquist, K. A. CD8 $\alpha\alpha$ intraepithelial lymphocytes arise from two main thymic precursors. *Nat. Immunol.* **18**, 771–779 (2017).
4. Leishman, A. J. et al. Precursors of functional MHC Class I- or Class II- restricted CD8 $\alpha\alpha$ ⁺ T cells are positively selected in the thymus by agonist self-peptides. *Immunity* **16**, 355–364 (2002).
5. Mayans, S. et al. abT Cell receptors expressed by CD4 $^+$ CD8b $^-$ intraepithelial T cells drive their fate into a unique lineage with unusual MHC reactivities. *Immunity* **41**, 207–218 (2014).
6. Poussier, P. A unique subset of self-specific inraintestinal T cells maintains gut integrity. *J. Exp. Med.* **195**, 1491–1497 (2002).
7. Olivares-Villagomez, D. et al. Thymus leukemia antigen controls intraepithelial lymphocyte function and inflammatory bowel disease. *Proc. Natl Acad. Sci. USA* **105**, 17931–17936 (2008).
8. Klose, C. S. N. et al. The transcription factor T-bet is induced by IL-15 and thymic agonist selection and controls CD8 $\alpha\alpha$. *Immunity* **41**, 230–243 (2014).
9. Hsieh, C.-S., Lee, H.-M. & Lio, C.-W. J. Selection of regulatory T cells in the thymus. *Nat. Rev. Immunol.* <https://doi.org/10.1038/nri3155> (2012).
10. Klein, L., Robey, E. A. & Hsieh, C. S. Central CD4. *Nat. Rev. Immunol.* 1–12 <https://doi.org/10.1038/s41577-018-0083-6> (2018).
11. Pobezinsky, L. A. et al. Clonal deletion and the fate of autoreactive thymocytes that survive negative selection. *Nat. Immunol.* **13**, 569–578 (2012).
12. Lio, C.-W. J. & Hsieh, C.-S. A two-step process for thymic regulatory T cell development. *Immunity* **28**, 100–111 (2008).
13. Burchill, M. A. et al. Linked T cell receptor and cytokine signaling govern the development of the regulatory T cell repertoire. *Immunity* **28**, 112–121 (2008).
14. Matsuda, J. L. et al. Homeostasis of Va14i NKT cells. *Nat. Immunol.* **3**, 966–974 (2002).
15. Marshall, D., Sinclair, C., Tung, S. & Seddon, B. Differential requirement for IL-2 and IL-15 during bifurcated development of thymic regulatory T cells. *J. Immunol.* **193**, 5525–5533 (2014).
16. Hu, D. Y., Wirasinha, R. C., Goodnow, C. C. & Daley, S. R. IL-2 prevents deletion of developing T-regulatory cells in the thymus. *Cell Death Differ.* **24**, 1007–1016 (2017).

17. Golec, D. P. et al. Thymic progenitors of TCR $\alpha\beta$ +CD8 $\alpha\alpha$ intestinal intraepithelial lymphocytes require RasGRP1 for development. *J. Exp. Med.* **214**, 2421–2435 (2017).
18. Ma, L. J., Acero, L. F., Zal, T. & Schluns, K. S. Trans-presentation of IL-15 by intestinal epithelial cells drives development of CD8 $\alpha\alpha$ IELs. *J. Immunol.* **183**, 1044–1054 (2009).
19. Lai, Y. G. et al. IL-15 does not affect IEL development in the thymus but regulates homeostasis of putative precursors and mature CD8 $^+$ IELs in the intestine. *J. Immunol.* **180**, 3757–3765 (2008).
20. Oh-hora, M. et al. Agonist-selected T cell development requires strong T cell receptor signaling and store-operated calcium entry. *Immunity* **38**, 881–895 (2013).
21. Klose, C. S., Hummel, J. F., Faller, L., d'Hargues, Y., Ebert, K. et al. A committed postselection precursor to natural TCR. *Mucosal Immunol.* 1–12, <https://doi.org/10.1038/mi.2017.54> (2017).
22. Melichar, H. J., Ross, J. O., Herzmark, P., Hogquist, K. A. & Robey, E. A. Distinct temporal patterns of T cell receptor signaling during positive versus negative selection in situ. *Sci. Signal.* **6**, 1–14 (2013).
23. Dzhagalov, I. L., Chen, K. G., Herzmark, P. & Robey, E. A. Elimination of self-reactive T cells in the thymus: a timeline for negative selection. *PLoS Biol.* **11**, e1001566 (2013).
24. Le Borgne, M. et al. The impact of negative selection on thymocyte migration in the medulla. *Nat Immunol.* **10**, 823–830 (2009).
25. Ross, J. O. et al. Distinct phases in the positive selection of CD8 $^+$ T cells distinguished by intrathymic migration and T-cell receptor signaling patterns. *Proc. Natl Acad. Sci. USA* **111**, E2550–E2558 (2014).
26. Weist, B. M., Kurd, N., Boussier, J., Chan, S. W. & Robey, E. A. Thymic regulatory T cell niche size is dictated by limiting IL-2 from antigen-bearing dendritic cells and feedback competition. *Nat. Immunol.* **16**, 635–641 (2015).
27. Kurd, N. S. et al. A role for phagocytosis in inducing cell death during thymocyte negative selection. *ELife* **8**, 1879 (2019).
28. Au-Yeung, B. B. et al. Quantitative and temporal requirements revealed for Zap70 catalytic activity during T cell development. *Nat. Immunol.* **15**, 687–694 (2014).
29. Ueda, Y. et al. mst1 regulates integrin-dependent thymocyte trafficking and antigen recognition in the thymus. *Nat. Commun.* **3**, 1098–1013 (2012).
30. Lancaster, J. N. et al. Live-cell imaging reveals the relative contributions of antigen-presenting cell subsets to thymic central tolerance. *Nat. Commun.* 1–15, <https://doi.org/10.1038/s41467-019-09727-4> (2019).
31. Ehrlich, L. I. R., Oh, D. Y., Weissman, I. L. & Lewis, R. S. Differential contribution of chemotaxis and substrate restriction to segregation of immature and mature thymocytes. *Immunity* **31**, 986–998 (2009).
32. Bhakta, N. R., Oh, D. Y. & Lewis, R. S. Calcium oscillations regulate thymocyte motility during positive selection in the three-dimensional thymic environment. *Nat. Immunol.* **6**, 143–151 (2005).
33. Wirasinha, R. C. et al. Deletion of self-reactive CCR7 $^-$ thymocytes in the absence of MHC expression on thymic epithelial cells. *Cell Death Differ.* 1–13, <https://doi.org/10.1038/s41418-019-0331-8> (2019).
34. McGargill, M. A. & Hogquist, K. A. Antigen-induced coreceptor down-regulation on thymocytes is not a result of apoptosis. *J. Immunol.* **162**, 1237–1245 (1999).
35. Shires, J., Theodoridis, E. & Hayday, A. C. Biological Insights Into TCRg δ ⁺ and TCR $\alpha\beta$ ⁺ intraepithelial lymphocytes provided by Serial Analysis of Gene Expression (SAGE). *Immunity* **15**, 419–434 (2001).
36. Denning, T. L. et al. Mouse TCR $\alpha\beta$ +CD8 $\alpha\alpha$ intraepithelial lymphocytes express genes that down-regulate their antigen reactivity and suppress immune responses. *J. Immunol.* **178**, 4230–4239 (2007).
37. Yamagata, T., Benoist, C. & Mathis, D. A shared gene-expression signature in innate-like lymphocytes. *Immunity. Rev.* **210**, 1–15 (2006).
38. Daniels, M. A. et al. Thymic selection threshold defined by compartmentalization of Ras/MAPK signalling. *Nature* **444**, 724–729 (2006).
39. Stoklasek, T. A., Schluns, K. S. & Lefrancois, L. Combined IL-15/IL-15R immunotherapy maximizes IL-15 activity in vivo. *J. Immunol.* **177**, 6072–6080 (2006).
40. Dubois, S., Mariner, J., Waldmann, T. A. & Tagaya, Y. IL-15Ra recycles and presents IL-15 in trans to neighboring cells. *Immunity* **17**, 537–547 (2002).
41. Burkett, P. R. et al. Coordinate expression and trans presentation of Interleukin (IL)-15Ra and IL-15 supports natural killer cell and memory CD8 $^+$ T cell homeostasis. *J. Exp. Med.* **200**, 825–834 (2004).
42. Boyman, O., Kovar, M., Rubenstein, M. P., Surh, C. D. & Sprent, J. Selective stimulation of T cell subsets with antibody-cytokine immune complexes. *Science* **311**, 1921–1924 (2006).
43. Nikolic-Zugic, J. & Carbone, F. R. The effect of mutations in the MHC class I peptide binding groove on the cytotoxic T lymphocyte recognition of the K b -restricted ovalbumin determinant. *Eur. J. Immunol.* **20**, 2431–2437 (1990).
44. Hsieh, C.-S., Zheng, Y., Liang, Y., Fontenot, J. D. & Rudensky, A. Y. An intersection between the self-reactive regulatory and nonregulatory T cell receptor repertoires. *Nat. Immunol.* **7**, 401–410 (2006).

45. Sinclair, C., Bains, I., Yates, A. J. & Seddon, B. Asymmetric thymocyte death underlies the CD4:CD8 T-cell ratio in the adaptive immune system. *Proc. Natl Acad. Sci. USA* **110**, E2905–E2914 (2013).
46. Legoux, F. P. et al. T cell tolerance to tissue-restricted self antigens is mediated by antigen-specific regulatory T cells rather than deletion. *Immunity* **43**, 896–908 (2015).
47. Malhotra, D. et al. Tolerance is established in polyclonal CD4⁺ T cells by distinct mechanisms, according to self-peptide expression patterns. *Nat. Immunol.* **17**, 187–195 (2016).
48. Koehli, S., Naeher, D., Galati-Fournier, V., Zehn, D. & Palmer, E. Optimal T-cell receptor affinity for inducing autoimmunity. *Proc. Natl Acad. Sci. USA* **111**, 17248–17253 (2014).
49. Fife, B. T. et al. Interactions between PD-1 and PD-L1 promote tolerance by blocking the TCR-induced stop signal. *Nat. Immunol.* **10**, 1185–1192 (2009).
50. Koble, C. & Kyewski, B. The thymic medulla: a unique microenvironment for self-antigen transfer. *J. Exp. Med.* **206**, 1505–1513 (2009).
51. Cui, G. et al. Characterization of the IL-15 niche in primary and secondary lymphoid organs in vivo. *Proc. Natl Acad. Sci. USA* **111**, 1915–1920 (2014).
52. Owen, D. L. et al. Identification of cellular sources of IL-2 needed for regulatory T cell development and homeostasis. *J. Immunol.* **200**, 3927–3933 (2018).
53. Konkel, J. E. et al. Control of the development of CD8 $\alpha\alpha$. *Nat. Immunol.* **12**, 312–319 (2011).
54. Mamelaki, C. et al. Thymic depletion and peripheral activation of class. *Proc. Natl Acad. Sci. USA* **89**, 11342–11346 (1992).
55. Lindquist, R. L. et al. Visualizing dendritic cell networks in vivo. *Nat. Immunol.* **5**, 1243–1250 (2004).
56. Gardner, J. M. et al. Deletional tolerance mediated by extrathymic aire-expressing cells. *Science*. **321**, 843–847 (2008).
57. Dzhagalov, I. L., Melichar, H. J., Ross, J. O., Herzmark, P. & Robey, E. A. Two-photon imaging of the immune system. *Curr. Protocol Cytometry*. **60**, 12.26.1–12.26.20 (2012).
58. Halkias, J. et al. Opposing chemokine gradients control human thymocyte migration in situ. *J. Clin. Invest.* **123**, 2131–2142 (2013).